

Rare charm decays at LHCb

Marco Colonna^{a*} on behalf of the LHCb collaboration

^a*Technische Universität Dortmund,
Dortmund, Germany*

E-mail: marco.colonna@cern.ch

The LHCb experiment collected the world's largest sample of charmed hadron decays. This data set allowed the LHCb collaboration to provide the most precise results for rare charm decays with two leptons in the final states. This document presents the latest results from the LHCb collaboration on charmed mesons and baryons rare decays.

*Discrete 2024,
02-06 December 2024,
Ljubljana, Republika Slovenija*

*Speaker

© Copyright owned by the author(s) under the terms of the Creative Commons Attribution-NonCommercial-NoDerivatives 4.0 International License (CC BY-NC-ND 4.0). All rights for text and data mining, AI training, and similar technologies for commercial purposes, are reserved. ISSN 1824-8039. Published by SISSA Medialab.

<https://pos.sissa.it/>

1. Introduction

Rare decays involving transitions between c and u quarks, with the emission of a pair of oppositely charged leptons, provide a valuable opportunity to study flavor-changing neutral-currents (FCNCs) in the up-type quark sector. In the Standard Model (SM), FCNC transitions occur only through loop-level processes and are heavily suppressed by the Glashow–Iliopoulos–Maiani (GIM) mechanism [1]. For the charm system, the GIM mechanism imposes an exceptionally strong suppression compared to the down-type quark sector. Due to the strong suppression of FCNC mediated processes the amplitude of the $c \rightarrow u\ell^+\ell^-$ transitions is dominated by intermediate hadronic-resonance processes. Rare charm decays are however a sensitive probe for physics beyond the Standard Model [2].

Different approaches can be used to investigate rare charm decays with two oppositely charged leptons in the final state. The first method is measuring the branching fraction (\mathcal{B}) of the FCNC-mediated decays in the dilepton mass ($m_{\ell\ell}$) regions of the phase-space which are not dominated by the hadronic-resonance mediated decays [3, 4]. The second method is to search in the resonant dominated regions, performing null tests such as the CP asymmetry and the forward-backward (FB) asymmetry of the lepton system. In fact these observables are expected to vanish in the SM and NP contributions might interfere with the resonant modes of the decay leading these observables to deviate from zero [5, 6, 7, 8]. Finally it is possible to investigate NP by performing lepton-flavour-universality (LFU) tests by comparing the branching fraction of the decay modes with muons, and electrons, in the final state [9, 10, 11, 12]. The following sections present the most recent results obtained by the LHCb collaboration, using all three of these approaches.

2. Search for $\Lambda_c^+ \rightarrow p\mu^+\mu^-$ decays

The measurement of the \mathcal{B} of the $\Lambda_c^+ \rightarrow p\mu^+\mu^-$ decay has been performed at LHCb using a sample of proton-proton collisions, recorded between 2016 and 2018, corresponding to an integrated luminosity of 5.4 fb^{-1} [13].

The analysis is performed by dividing the dilepton mass spectrum, distinguishing between different resonant dominated regions defined according to the expected intermediate resonance: (low mass) $211-508 \text{ MeV}/c^2$, (η) $508-588 \text{ MeV}/c^2$, (ω) $743-823 \text{ MeV}/c^2$, (ρ) $588-743$ or $823-965 \text{ MeV}/c^2$, (ϕ) $979-1059 \text{ MeV}/c^2$ and (high mass) $1059-1348 \text{ MeV}/c^2$. The non resonant region is defined as the joint of the low mass and high mass regions. The branching fraction is defined with respect to the $\Lambda_c^+ \rightarrow p[\mu^+\mu^-]_\phi$ normalization mode as:

$$\mathcal{B}(\Lambda_c^+ \rightarrow p\mu^+\mu^-) = \frac{N(\Lambda_c^+ \rightarrow p\mu^+\mu^-)}{N(\Lambda_c^+ \rightarrow p[\mu^+\mu^-]_\phi)} \times \frac{\epsilon(\Lambda_c^+ \rightarrow p[\mu^+\mu^-]_\phi)}{\epsilon(\Lambda_c^+ \rightarrow p\mu^+\mu^-)} \times \mathcal{B}(\Lambda_c^+ \rightarrow p\phi) \times \mathcal{B}(\phi \rightarrow \mu^+\mu^-) \quad (1)$$

where N is the observed yield of the contributions and ϵ is the efficiency of reconstruction, and selection. The branching fraction is measured separately in all the dilepton mass regions.

The signal candidates are selected online via exclusive high-level trigger selection and offline with a preliminary cut based selection, followed by two consecutive multivariate analysis; the first

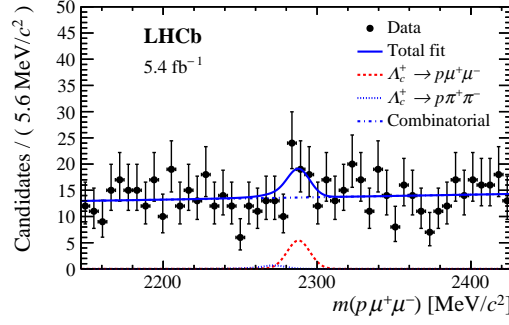


Figure 1: Mass distributions of selected $\Lambda_c^+ \rightarrow p\mu^+\mu^-$ candidates in the non-resonant dilepton mass region [13].

Table 1: Branching fractions of $\Lambda_c^+ \rightarrow p\mu^+\mu^-$ decays in different ranges of dimuon mass, where the uncertainties are statistical, systematic and due to the limited knowledge of the normalization branching fraction. The reported upper limits correspond to 90% (95%) confidence level [13].

$m(e^+e^-)$ region	$m(e^+e^-)$ [MeV/ c^2]	\mathcal{B}
	$\Lambda_c^+ \rightarrow p\mu^+\mu^-$	
Low mass	211–508	$< 0.93 (1.1) \times 10^{-8}$
η	508–588	$(1.67 \pm 0.69 \pm 0.23 \pm 0.34) \times 10^{-3}$
ω	743–823	$(9.82 \pm 1.23 \pm 0.73 \pm 2.79) \times 10^{-4}$
ρ^0	588-743 or 823-965	$(1.52 \pm 0.34 \pm 0.14 \pm 0.24) \times 10^{-3}$
High mass	> 1100	$< 3.0 (3.3) \times 10^{-8}$
Non resonant	211-508 or >1100	$< 2.9 (3.2) \times 10^{-8}$

based on the topological and kinematic variables of the Λ_c^+ candidates, the second including also kinematic, vertex and isolation variables related to the final state particles. The selection is finalized by imposing particle identification (PID) requirements on both the proton and the muons in the final state.

The yields are measured with unbinned maximum likelihood fits to the Λ_c^+ invariant mass distributions. In the dilepton mass regions where the invariant mass distribution is compatible with the background only hypothesis 90% and 95% C.L. upper limits for the branching fraction are established. The Λ_c^+ invariant mass spectrum in the non-resonant dilepton mass region is shown in Fig. 1. The results are summarized in Tab. 1.

Assuming a decay model with the final state particles uniformly distributed in the phase-space it is possible to infer an upper limit for the \mathcal{B} of the non-resonant $\Lambda_c^+ \rightarrow p\mu^+\mu^-$ decay over all the dilepton mass phase-space as $\mathcal{B}(\Lambda_c^+ \rightarrow p\mu^+\mu^-) < 7.3 (8.2) \times 10^{-8}$ at 90% (95%) CL [13].

3. Search for resonance enhanced asymmetries in $\Lambda_c^+ \rightarrow p\mu^+\mu^-$ decays

The first measurement of direct CP asymmetry, CP average and CP asymmetry of the FB asymmetry in the lepton system, in the $\Lambda_c^+ \rightarrow p\mu^+\mu^-$ decay has been performed at LHCb [14]. The same sample described in Section 2 has been used, but the candidates' selection has been optimized differently according to the aim of the measurement.

Table 2: Yields after correcting for relative efficiency variations and measured asymmetries for $\Lambda_c^+ \rightarrow p\mu^+\mu^-$ decays in the two dimuon-mass regions. For the asymmetries the first uncertainty is statistical and the second systematic [14].

$m(\mu^+\mu^-)$	Efficiency-weighted yields			Asymmetries		
	Signal	Misid. back.	Comb. back.	A_{CP} [%]	ΣA_{FB}^{CP} [%]	ΔA_{FB}^{CP} [%]
ϕ_{low}	346 ± 22	57 ± 21	437 ± 26	$-0.8 \pm 6.2 \pm 0.6$	$6.9 \pm 6.1 \pm 1.0$	$4.8 \pm 6.1 \pm 0.8$
ϕ_{high}	435 ± 22	35 ± 17	390 ± 25	$-1.4 \pm 5.3 \pm 0.6$	$1.6 \pm 5.2 \pm 0.8$	$1.9 \pm 5.2 \pm 0.6$

The CP asymmetry, A_{CP} , is defined in terms of the difference of decay rates for Λ_c^+ and $\bar{\Lambda}_c^-$ as:

$$A_{CP} \equiv \frac{\Gamma(\Lambda_c^+ \rightarrow p\mu^+\mu^-) - \Gamma(\bar{\Lambda}_c^- \rightarrow \bar{p}\mu^+\mu^-)}{\Gamma(\Lambda_c^+ \rightarrow p\mu^+\mu^-) + \Gamma(\bar{\Lambda}_c^- \rightarrow \bar{p}\mu^+\mu^-)}, \quad (2)$$

where Γ is the decay rate. The forward-backward asymmetry, A_{FB} , is defined as

$$A_{FB} \equiv \frac{\Gamma(\cos\theta > 0) - \Gamma(\cos\theta < 0)}{\Gamma(\cos\theta > 0) + \Gamma(\cos\theta < 0)}, \quad (3)$$

where θ is the angle between the direction of the same-sign lepton, with respect to the initial state baryon, in the dimuon rest frame and the flight direction of the dimuon system in the rest frame of the baryon.

The CP asymmetry is measured in two dilepton mass bins in the ϕ -resonance dominated dilepton mass spectrum: (ϕ -low) 979 – 1019 MeV/ c^2 and (ϕ -high) 1019 – 1059 MeV/ c^2 . The FB asymmetry is measured in the same dilepton mass bins, also distinguishing between the two flavours of the initial state particle (Λ_c^+ and $\bar{\Lambda}_c^-$), and the results are combined as:

$$\Sigma A_{FB}^{CP} = 1/2 \cdot \left[A_{FB}^{\Lambda_c^+} + A_{FB}^{\bar{\Lambda}_c^-} \right] \quad (4)$$

$$\Delta A_{FB}^{CP} = 1/2 \cdot \left[A_{FB}^{\Lambda_c^+} - A_{FB}^{\bar{\Lambda}_c^-} \right] \quad (5)$$

further increasing the sensitivity to the real and imaginary parts of NP couplings.

The Λ_c^+ candidates are selected requiring three tracks, compatible with the baryon decay vertex, and exceeding transverse momentum thresholds. Furthermore the Λ_c^+ reconstructed momentum is required to be in the direction aligned with the primary vertex of the event. A tight requirement on the PID variable of the proton has been applied to suppress the $D^+ \rightarrow \pi^+\mu^+\mu^-$ misidentified channel, where the pion is identified as proton. A multivariate analysis, based on kinematic, topological features and features related to the isolation of the signal candidates with respect to other tracks in the event, has been used to further suppress the combinatorial background. The cut on the multivariate variable has been optimized together with the requirements on the PID of the muons. Possible acceptance effects on the reconstruction and selection of the candidates have been corrected through a reweighting scheme based on simulations. Instrumental asymmetries have been subtracted to the signal A_{CP} by using the cabibbo favoured $\Lambda_c^+ \rightarrow pK_s^0$ decay as control channel.

The yields, and the asymmetries, are measured with unbinned maximum likelihood fits to the Λ_c^+ invariant mass distribution, which spectrum is shown in Fig. 2. The results from the fit are summarized in Tab. 2.

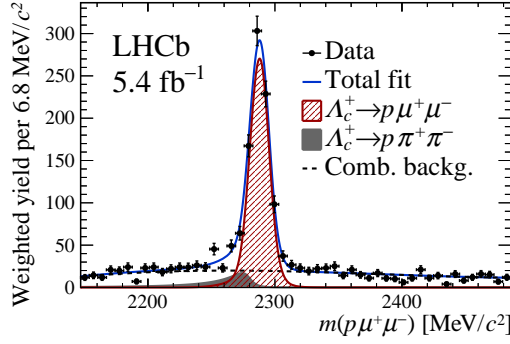


Figure 2: Distribution of $m(p\mu^+\mu^-)$ for efficiency-weighted candidates, together with the fit projection [14].

The dimuon-mass integrated values of A_{CP} , ΣA_{FB}^{CP} and ΔA_{FB}^{CP} , have been computed as the weighted average of the results in the two dilepton mass bins, coherently taking into account the correlation among the systematic uncertainties [15], and found to be:

$$\begin{aligned} A_{CP} &= (-1.1 \pm 4.0 \pm 0.5)\% \\ \Sigma A_{FB}^{CP} &= (3.9 \pm 4.0 \pm 0.6)\% \\ \Delta A_{FB}^{CP} &= (3.1 \pm 4.0 \pm 0.4)\% \end{aligned}$$

The results of the null-tests are compatible with a Standard Model scenario.

4. Search for $D^0 \rightarrow h^+h^-e^+e^-$ decays

The semileptonic rare charm decay $D^0 \rightarrow \pi^+\pi^-e^+e^-$ observed has been for the first time at LHCb [16] using a sample of proton-proton collisions, recorded between 2015 and 2018, corresponding to an integrated luminosity of 6 fb^{-1} . The $D^0 \rightarrow K^+K^-e^+e^-$ decay has been also studied at LHCb, and the current world best upper limit on its branching fraction has been established. The analysis has been performed over the spectrum of the dilepton mass, distinguishing between different resonant dominated regions defined according to the expected intermediate resonance: (low mass) $211 - 525 \text{ MeV}/c^2$, (η) $525 - 565 \text{ MeV}/c^2$, (ρ^0/ω) $565 - 950 \text{ MeV}/c^2$, (ϕ) $950 - 1100 \text{ MeV}/c^2$ and (high mass) $> 1100 \text{ MeV}/c^2$ for the $D^0 \rightarrow \pi^+\pi^-e^+e^-$ channel; (low mass) $211 - 525 \text{ MeV}/c^2$, (η) $525 - 565 \text{ MeV}/c^2$ and (ρ^0/ω) $> 565 \text{ MeV}/c^2$ for the $D^0 \rightarrow K^+K^-e^+e^-$ channel. The branching fraction is defined with respect to the $D^0 \rightarrow K^+\pi^-e^+e^-$ normalization mode as:

$$\begin{aligned} \mathcal{B}(D^0 \rightarrow h^+h^-e^+e^-) &= \frac{N(D^0 \rightarrow h^+h^-e^+e^-)}{N(D^0 \rightarrow K^-\pi^+[e^+e^-]_{\rho^0\omega})} \times \frac{\epsilon(D^0 \rightarrow K^-\pi^+[e^+e^-]_{\rho^0\omega})}{\epsilon(D^0 \rightarrow h^+h^-e^+e^-)} \\ &\quad \times \mathcal{B}(D^0 \rightarrow K^-\pi^+[e^+e^-]_{\rho^0\omega}) \quad (6) \end{aligned}$$

where the symbols definition is the same of Equation 1. The D^0 candidates are required to originate from a preceding $D^{*+} \rightarrow D^0\pi^+$ decay by cutting in a narrow region of $3 \text{ MeV}/c^2$ of the mass difference $\Delta m = m(D^{*+}) - m(D^0)$. This allows to reduce significantly the combinatorial background. A multivariate analysis, based kinematic and reconstruction quality features, is applied

Table 3: Branching fractions of (top) $D^0 \rightarrow \pi^+\pi^-e^+e^-$ and (bottom) $D^0 \rightarrow K^+K^-e^+e^-$ decays in different ranges of dielectron mass, where the uncertainties are statistical, systematic and due to the limited knowledge of the normalization branching fraction. The reported upper limits correspond to 90% (95%) confidence level.

$m(e^+e^-)$ region	$m(e^+e^-)$ [MeV/ c^2]	\mathcal{B} [10^{-7}]
$D^0 \rightarrow \pi^+\pi^-e^+e^-$		
Low mass	211–525	< 4.8 (5.4)
η	525–565	< 2.3 (2.7)
ρ^0/ω	565–950	$4.5 \pm 1.0 \pm 0.7 \pm 0.6$
ϕ	950–1100	$3.8 \pm 0.7 \pm 0.4 \pm 0.5$
High mass	> 1100	< 2.0 (2.2)
Total	–	$13.3 \pm 1.1 \pm 1.7 \pm 1.8$
$D^0 \rightarrow K^+K^-e^+e^-$		
Low mass	$2m_\mu$ –525	< 1.0 (1.1)
η	525–565	< 0.4 (0.5)
ρ^0/ω	> 565	< 2.2 (2.5)

to further distinguish signal from background. A multivariate electron-identification discriminant is used to further reduce the backgrounds originating from the hadronic $D^0 \rightarrow \pi^+\pi^-\pi^+\pi^-$ and $D^0 \rightarrow K^+K^-\pi^+\pi^-$ decays, where two pions are misidentified as electrons.

The yields are measured with unbinned maximum likelihood fits to the D^0 invariant mass distributions. The branching fractions are measured only in dilepton mass regions where the signal statistical significance exceeds three standard deviations with respect to the only background hypothesis. In the other dilepton mass regions 90% and 95% C.L. upper limits are established. The integrated \mathcal{B} of the $D^0 \rightarrow \pi^+\pi^-e^+e^-$ decay has been also measured. The results are summarized in Tab. 3.

The results are consistent with the branching fractions of the $D^0 \rightarrow \pi^+\pi^-\mu^+\mu^-$ and $D^0 \rightarrow K^+K^-\mu^+\mu^-$ decays previously measured by LHCb, and confirm lepton universality at the current precision.

References

- [1] S. L. Glashow, J. Iliopoulos, and L. Maiani, *Weak Interactions with Lepton-Hadron Symmetry*, *Phys. Rev.* **D2**, 7.
- [2] Hector Gisbert, Gudrun Hiller, and Dominik Suelmann, *Effective field theory analysis of rare $|\Delta c| = |\Delta u| = 1$ charm decays*, *JHEP* **12**. arXiv: 2410.00115 [hep-ph].
- [3] Stefan Meinel, $\Lambda_c \rightarrow N$ form factors from lattice QCD and phenomenology of $\Lambda_c \rightarrow n\ell^+\nu_\ell$ and $\Lambda_c \rightarrow p\mu^+\mu^-$ decays, *Phys. Rev.* **D97**, 3. arXiv: 1712.05783 [hep-lat].
- [4] R. N. Faustov and V. O. Galkin, *Rare $\Lambda_c \rightarrow p\ell^+\ell^-$ decay in the relativistic quark model*, *Eur. Phys. J.* **C78**, 6. arXiv: 1805.02516 [hep-ph].

- [5] Svjetlana Fajfer and Sasa Prelovšek, *Effects of littlest Higgs model in rare D meson decays*, *Phys. Rev.* **D73**. arXiv: [hep-ph/0511048](#) [[hep-ph](#)].
- [6] Ikaros I. Bigi and Ayan Paul, *On CP asymmetries in two-, three- and four-body D decays*, *JHEP* **03**. arXiv: [1110.2862](#) [[hep-ph](#)],
- [7] Svjetlana Fajfer and Nejc Košnik, *Resonance catalyzed CP asymmetries in $D \rightarrow P\ell^+\ell^-$* , *Phys. Rev.* **D87**. arXiv: [1208.0759](#) [[hep-ph](#)].
- [8] Luigi Cappiello, Oscar Catà, and Giancarlo D'Ambrosio, *Standard model prediction and new physics tests for $D^0 \rightarrow h_1^+h_2^-\ell^+\ell^-$ ($h = \pi, K; \ell = e, \mu$)*, *JHEP* **04**. arXiv: [1209.4235](#) [[hep-ph](#)],
- [9] Stefan De Boer and Gudrun Hiller, *Null tests from angular distributions in $D \rightarrow P_1P_2l^+l^-$, $l = e, \mu$ decays on and off peak*, *Phys. Rev.* **D98**, 3. arXiv: [1805.08516](#) [[hep-ph](#)].
- [10] Rigo Bause et al., *The new physics reach of null tests with $D \rightarrow \pi\ell\ell$ and $D_s \rightarrow K\ell\ell$ decays*, *Eur. Phys. J.* **C80**, 1. arXiv: [1909.11108](#) [[hep-ph](#)].
- [11] Aoife Bharucha, Diogo Boito, and Cédric Méaux, *Disentangling QCD and new physics in $D^+ \rightarrow \pi^+\ell^+\ell^-$* , *JHEP* **04**. arXiv: [2011.12856](#) [[hep-ph](#)].
- [12] Svjetlana Fajfer, Eleftheria Solomonidi, and Luiz Vale Silva, *S-wave contribution to rare $D^0 \rightarrow \pi^+\pi^-\ell^+\ell^-$ decays in the standard model and sensitivity to new physics*, *Phys. Rev.* **D109**. arXiv: [2312.07501](#) [[hep-ph](#)].
- [13] LHCb Collaboration, *Search for the rare decay of charmed baryon Λ_c^+ into the $p\mu^+\mu^-$ final state*, *Phys. Rev. D* **110**, 5.
- [14] LHCb Collaboration, *Search for resonance-enhanced CP and angular asymmetries in the $\Lambda_c^+ \rightarrow p\mu^+\mu^-$ decay at LHCb*, 2025, arXiv: [2502.04013](#) [[hep-ex](#)],
- [15] Louis Lyons, Duncan Gibaut, and Peter Clifford, *How to combine correlated estimates of a single physical quantity*, *Nucl. Instrum. Meth.* **A270**.
- [16] LHCb Collaboration, *Search for D^0 meson decays to $\pi^+\pi^-e^+e^-$ and $K^+K^-e^+e^-$ final states*, arXiv: [2412.09414](#) [[hep-ex](#)].